

Structure of a Precursor State in Dissociative Chemisorption

R. McGrath, A. A. MacDowell, T. Hashizume,^(a) F. Sette, and P. H. Citrin

AT&T Bell Laboratories, Murray Hill, New Jersey 07974

(Received 30 October 1989)

Near-edge- and surface-extended-x-ray-absorption fine-structure measurements of H₂S on Cu(001)*p*(2×2)S have been used to make the first direct structural determination of an intermediate molecular precursor in dissociative adsorption. Our results indicate that population of these precursor states overcomes the kinetic barrier to H₂S adsorption and leads to the formation of a *c*(2×2)S structure.

PACS numbers: 78.70.Dm, 61.10.Lx, 68.45.-v, 82.65.-i

Molecules impinging on a single-crystal surface can desorb, diffuse, adsorb, or react depending on a variety of competing thermodynamical, statistical, and structural factors.¹ Recent progress has been made in theoretically modeling some of these kinetic processes,² offering the promise of elucidating part of a large body of related experimental work. These calculations and macroscopic measurements are of obvious value, but they are limited by the lack of microscopic experimental input concerning the individual surface processes. In particular, the central role of a molecular reaction intermediate or precursor state in determining the kinetics of adsorption has been difficult to establish, due largely to the absence of any detailed information about the structure of the precursor itself. Attempts to infer a precursor binding site or configuration have relied mainly on photoemission and electron energy-loss spectroscopies,³ and only recently has limited information been obtained⁴ using a specifically structural probe.

In this Letter, we use near-edge- and surface-extended-x-ray-absorption fine-structure (NEXAFS and SEXAFS) measurements to identify, isolate, and characterize a molecular precursor state in the dissociative adsorption of H₂S on Cu(001)*p*(2×2)S. Our temperature- and coverage-dependent data from the kinetically frozen precursor allow its configuration, binding site, and bonding distance to the substrate to be determined unambiguously. The system of H₂S on Cu(001)*p*(2×2)S was studied because it exhibits a kinetic barrier to adsorption whose origin has remained unknown: Unlike other H₂S-exposed metal (001) surfaces which dissociatively adsorb ~0.5 monolayer (ML) of S and form *c*(2×2) overlayers, e.g., Ni⁵ and Co,⁶ and the Cu(001) surface dosed with H₂S adsorbs only ≲0.25 ML of S in a *p*(2×2) structure. Based on our results, we show that it is the barrier to forming the molecular precursor state that is responsible for this phenomenon. Our findings clarify the process by which dissociation on this surface occurs and they suggest a mechanism for overcoming the barrier to H₂S adsorption. The novel application of these measurements to a metastable reaction intermediate demonstrates their utility in studying problems of surface kinetics.

Sulfur *K*-edge SEXAFS and NEXAFS data were measured with fluorescence-yield detection using the new AT&T Bell Laboratories X15B beam line⁷ at the National Synchrotron Light Source. The clean Cu(001) surface was exposed to H₂S either by backfilling the chamber to 5×10⁻⁸ Torr, giving a "low" impingement rate,⁸ or by using a directional doser with an estimated enhancement factor of >100, giving a "high" impingement rate. All data shown were measured from surfaces at 90 K, including those prepared initially at higher temperatures. Low-energy electron-diffraction (LEED) measurements were obtained only from room-temperature surfaces to minimize electron-stimulated desorption or dissociation of the H₂S overlayer(s).

NEXAFS measurements are used to determine the chemical identity, the amount, and the orientational order of the different adsorbed species. Figure 1(a) shows normal- and grazing-incidence spectra from a Cu(001)-*p*(2×2)S surface formed by dosing clean Cu(001) with ~5 L [1 L (langmuir) = 10⁻⁶ Torr] of H₂S at 300 K and a *low* impingement rate. Under these dosing conditions, exposures as high as 50000 L result in *no* additional H₂S adsorption and produce only this structure. The anisotropic peak at ≲2469 eV corresponds to transitions from S 1*s* states into unfilled *p*-derived hybrid states of S and Cu and is characteristic of ordered atomic S chemisorbed on metals.⁵ Previous measurements⁹⁻¹³ establish that this *p*(2×2) overlayer consists of 0.22±0.01 ML of S atoms occupying fourfold-hollow sites with a S-Cu bond length of 2.27±0.02 Å. The S-covered surface is also thought to undergo a small reconstruction, which is currently under debate.^{10,11} We denote the chemisorbed atomic species in this overlayer S(*c*).

The NEXAFS spectra obtained immediately after dosing the Cu(001)*p*(2×2)S surface with H₂S at 90 K and a *high* impingement rate are shown in Fig. 1(b). The data are now isotropic, indicative of a disordered system, and are much more intense. They closely resemble H₂S gas-phase [H₂S(*g*)] measurements in which the shifted peak at ~2472 eV corresponds to transitions into the antibonding σ* molecular orbital of the S-H bond.¹⁴ The identification of this species as physisorbed H₂S, denoted H₂S(*p*), is confirmed from the residual-gas

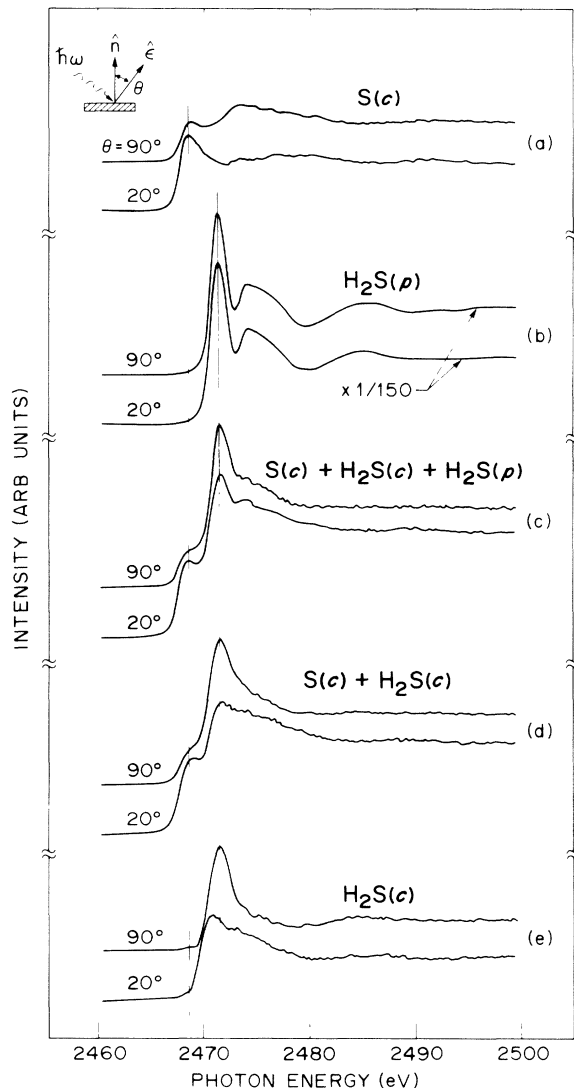


FIG. 1. S K -edge NEXAFS data from Cu(001) surfaces dosed with H_2S at low and high impingement rates (see text and Ref. 8). (a) Low H_2S dosing of clean Cu(001) at 300 K gives atomic chemisorbed species, $\text{S}(c)$, with a $p(2 \times 2)$ LEED pattern. (b) High H_2S dosing at 90 K of surface in (a) gives a multilayer film of molecular physisorbed species, $\text{H}_2\text{S}(p)$. (c) Low H_2S dosing at 90 K of surface in (a) gives much less adsorbed H_2S . Shown are data for the surface after ~ 1 -h exposure in the photon beam. (d) Several hours additional exposure desorbs $\text{H}_2\text{S}(p)$, leaving a stable surface of initial $\text{S}(c)$ plus a new molecular chemisorbed species, $\text{H}_2\text{S}(c)$. (e) $\text{H}_2\text{S}(c)$ is isolated by subtracting spectra in (a) from those in (d).

analysis of H_2S , which was observed to evaporate from this 90-K film over a period of ~ 30 min. The thickness of the $\text{H}_2\text{S}(p)$ layer in Fig. 1(b) is estimated to be ~ 50 ML using the edge jump from the 0.22-ML $p(2 \times 2)\text{S}$ structure as a calibration.

If the $p(2 \times 2)\text{S}$ surface in Fig. 1(a) is dosed at 90 K using a low impingement rate of H_2S , the NEXAFS

spectra shown in Fig. 1(c) are obtained. [These data are similar to those after most of the $\text{H}_2\text{S}(p)$ film in Fig. 1(b) has evaporated at 90 K.] The spectral intensity from $\text{S}(c)$ is now apparent because the contribution from the adsorbed H_2S , determined here to be ~ 0.26 ML, is much smaller. Several hours of exposure to the photon beam leads to photodesorption of ~ 0.06 ML of H_2S and a resulting surface, see Fig. 1(d), which is stable at 90 K. The remaining 0.2 ML of H_2S is shown below to be chemisorbed and is denoted $\text{H}_2\text{S}(c)$. The $\text{H}_2\text{S}(c)$ contribution is isolated from that of the coexisting $\text{S}(c)$ species by taking the difference between the spectra in Figs. 1(d) and 1(a); see Fig. 1(e). Note that aside from its lower intensity relative to the $\text{H}_2\text{S}(p)$ data, the σ^* resonance in the $\text{H}_2\text{S}(c)$ data is anisotropic and has a sense opposite to the $\text{S}(c)$ spectra in Fig. 1(a). Since dipole-allowed transitions from $\text{S } 1s \rightarrow \text{S-H } \sigma^*$ will be maximized when the photon electric field $\hat{\epsilon}$ lies within the H-S-H plane and perpendicular to the c_2 axis, the observed anisotropy of the σ^* resonance indicates that the $\text{H}_2\text{S}(c)$ molecule is oriented with its reflection axis along or close to the surface normal.

More detailed structural information about $\text{H}_2\text{S}(c)$ is obtained using SEXAFS measurements. Figure 2(a) displays normal-incidence background-subtracted SEXAFS data, $\chi(k)$, and their Fourier transform (FT), measured from the $\text{Cu}(001)p(2 \times 2)\text{S}$ surface of Fig. 1(a). Identically analyzed data in Fig. 2(b) are from the H_2S -dosed stable surface of Fig. 1(d). The amplitude of the first-shell FT peak is much smaller in Fig. 2(b) primarily because it represents the sum of two different (interfering) first-neighbor distances,¹⁵ one from the $\text{S}(c)$ -Cu bond at $r_1 = 2.27$ Å in the $p(2 \times 2)\text{S}$ structure and the other from the $\text{H}_2\text{S}(c)$ -Cu bond at r'_1 in a structure to be determined (the H atoms contribute negligible SEXAFS). We isolate the SEXAFS originating from the $\text{H}_2\text{S}(c)$ alone (as we did in the NEXAFS data) by subtracting the contribution of $\text{S}(c)$. The resulting $\chi(k)$ and FT data are shown in Fig. 2(c). Using standard EXAFS analysis procedures,¹⁶ r'_1 is determined to be 2.38 ± 0.04 Å, where the uncertainty includes possible systematic errors in the subtraction. The measured SEXAFS first-neighbor amplitudes at grazing incidence (not shown) and normal incidence give a ratio of effective coordination numbers $N'_g/N'_n = 1.4 \pm 0.2$, which compares very well with the value of 1.42 calculated for $\text{H}_2\text{S}(c)$ occupying the fourfold-hollow site at 2.38 Å. Confirmation of our findings comes both from a least-squares fit of the unsubtracted raw data in Fig. 2(b), which gives results in excellent agreement with those obtained using the difference procedure, and from analysis of higher-neighbor shells;¹³ e.g., a third-neighbor distance at $r_3 \approx a_0(\text{Cu})$ due to $\text{H}_2\text{S}(c)$ - $\text{S}(c)$ scattering in fourfold sites (see Fig. 2 inset) is found in the data in Figs. 2(b) and 2(c) but not in Fig. 2(a). The structure of $\text{H}_2\text{S}(c)$ on $\text{Cu}(001)p(2 \times 2)\text{S}$ is thus an overall $c(2 \times 2)$ system consisting of two interwoven $p(2 \times 2)$

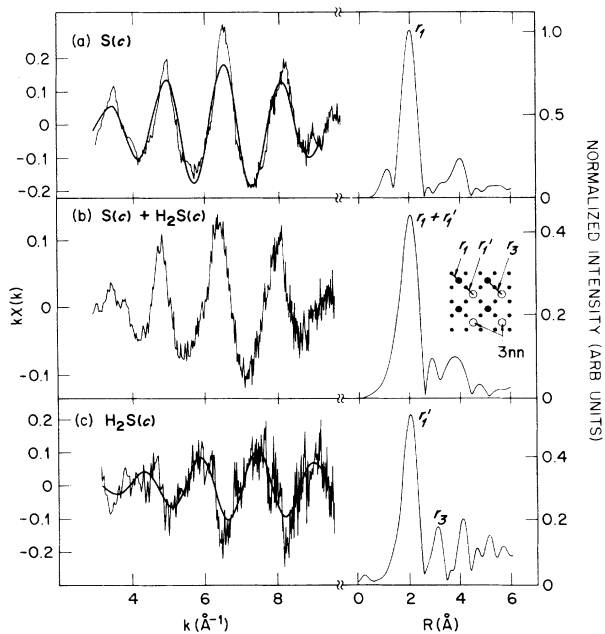


FIG. 2. Normal-incidence S K -edge SEXAFS data $\chi(k)$, and corresponding Fourier transforms, from Cu(001) surfaces dosed with H_2S . Note different scales. Apart from noise, differences between raw background-subtracted data and the solid line, which is the filtered first-nearest-neighbor (nn) shell r_1 or r_1' , are due to contributions from higher- nn shells (these are unlabeled in the FT data except for r_3 ; see Refs. 12 and 13 for details). (a) Cu(001) $p(2\times 2)$ S surface, as in Fig. 1(a). (b) Stable surface after H_2S dosing, as in Fig. 1(d). (c) Difference between raw data in (b) and (a) for isolating $\text{H}_2\text{S}(c)$ species, as in Fig. 1(e). Inset: $c(2\times 2)$ overlayer composed of S(c) (solid circles) and $\text{H}_2\text{S}(c)$ (open circles), each in $p(2\times 2)$ meshes. In the adsorbate coordination sphere, the first- nn site (unoccupied) is at distance $a_0/\sqrt{2}$, the second- nn site is at a_0 ($=r_3$), and the third- nn site (labeled) is at $\sqrt{2}a_0$.

meshes of chemisorbed S atoms and chemisorbed H_2S molecules, each in fourfold-hollow sites, with $\text{H}_2\text{S}(c)$ bonding S-end down to a Cu at a distance 0.1 \AA longer than that of S(c).

We now examine the role of $\text{H}_2\text{S}(c)$ in the dissociation of H_2S . Figure 3 shows a series of grazing-incidence NEXAFS scans taken after a freshly dosed $p(2\times 2)$ S surface [as in Fig. 1(c)] is successively annealed to the temperatures indicated. Warming the surface from 90 to 125 K desorbs $\text{H}_2\text{S}(p)$ and leaves the concentration of S(c) unchanged, similar to the $\text{H}_2\text{S}(p)$ photodesorption seen in going from Fig. 1(c) to Fig. 1(d). The remaining H_2S species is more strongly bound, i.e., chemisorbed, and is denoted $\text{H}_2\text{S}(c)$. As the temperature increases to 210 K, some of the $\text{H}_2\text{S}(c)$ desorbs, indicated by the smaller edge jump, while some of the $\text{H}_2\text{S}(c)$ dissociates, indicated by the loss of $\text{H}_2\text{S}(c)$ intensity and the concurrent growth of S(c) intensity. Annealing above 210 K results in still more dissociation. The LEED pattern from the surface warmed to 290 K is a diffuse $c(2\times 2)$

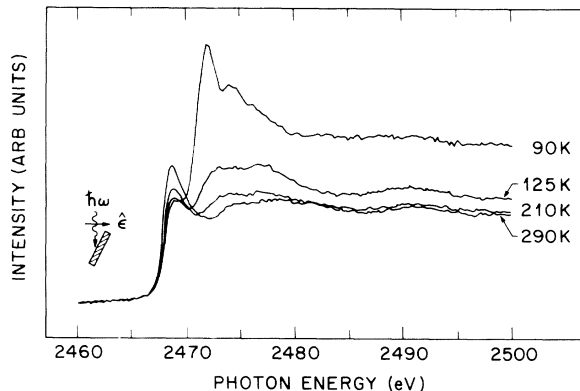
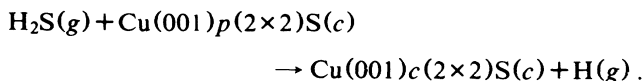


FIG. 3. S K -edge NEXAFS data from H_2S -dosed Cu(001)- $p(2\times 2)$ S surface [similar to Fig. 1(c)] as a function of temperature. All data were measured after cooling surfaces back to 90 K. Between 90 and 125 K, $\text{H}_2\text{S}(p)$ desorbs with little change of S(c), leaving the surface similar to that in Fig. 1(d). As the temperature increases, some $\text{H}_2\text{S}(c)$ desorbs while the S(c) species grows at the expense of $\text{H}_2\text{S}(c)$, i.e., $\text{H}_2\text{S}(c) \rightarrow \text{S}(c) + \text{H}(g)$.

pattern, identical to the one reported in a recent study⁹ of Cu(001) chemisorbed with a saturation coverage of 0.35–0.38 ML of S.¹⁷ The $c(2\times 2)$ S surface in Ref. 9 was prepared by high-temperature diffusion of S from the bulk. We have also obtained an identical surface at 300 K by predissociating H_2S at a low impingement rate using a hot W filament.¹³ The data in Fig. 3, combined with the fact that adsorption of atomic S leads to the same $c(2\times 2)$ S surface as that obtained from annealing the $\text{H}_2\text{S}(c)$ species on Cu(001) $p(2\times 2)$ S, directly demonstrate that $\text{H}_2\text{S}(c)$ is the precursor state to dissociation on that surface.

The above results lead to a number of conclusions about the surface reaction



There are two activation barriers controlling the rate of this reaction, both of which center around the precursor state identified here. One of these is simply the thermal barrier to dissociating $\text{H}_2\text{S}(c)$. Compared with the S-H bonds in $\text{H}_2\text{S}(g)$, those in the kinetically frozen $\text{H}_2\text{S}(c)$ precursor are expected to be weakened by the formation of new bonds between the S and the Cu(001) surface atoms. This bond weakening, which is facilitated by orienting the molecule S-end down, makes the barrier to H dissociation more accessible, but not quite enough in going from 90 to 125 K. Additional thermal energy is required to populate the higher vibrational states that lead to the actual breaking of S-H bonds. The final formation of the $c(2\times 2)$ S structure is further facilitated by having the $\text{H}_2\text{S}(c)$ species already in the required sites; i.e., there is no need for surface diffusion of the dissociat-

ed S. The process that does compete with $\text{H}_2\text{S}(c)$ dissociation, however, is desorption. Warming the surface weakens the already lengthened $\text{H}_2\text{S}(c)$ -Cu(001) bonds [relative to $\text{S}(c)$ -Cu(001)], explaining why some $\text{H}_2\text{S}(c)$ is observed to desorb in Fig. 3.

The second activation barrier involves *forming* the $\text{H}_2\text{S}(c)$ precursor. That such a barrier exists is evident from the fact that at 300 K and low H_2S impingement the $p(2\times 2)\text{S}$ surface does not adsorb any additional H_2S and evolve into a $c(2\times 2)\text{S}$ structure, whereas dosing with atomic S leads directly to this structure. The nature of this barrier, unlike that for thermally activated dissociation, is less obvious. From an energetic point of view, a model¹⁸ which assumes pairwise forces between adsorbates that are strongly repulsive for first nearest neighbors (nn), weakly repulsive for second nn, and weakly attractive for third nn would attribute the inhibited evolution of a $c(2\times 2)\text{S}$ structure at room temperature to the dominance of second-nn repulsions. From a structural point of view, however, the small S-induced reconstruction suggested to occur in the $p(2\times 2)\text{S}$ system^{10,11} might also be a factor in inhibiting the H_2S adsorption that leads to forming the $\text{H}_2\text{S}(c)$ state.

Based on our results and these considerations, we propose the following picture of how the barrier to $\text{H}_2\text{S}(c)$ formation is overcome. At low temperature, i.e., under conditions of slow surface diffusion, the formation of $\text{H}_2\text{S}(c)$ involves the adsorption of (at least) two H_2S molecules in nearest available fourfold-hollow sites. These sites are third nn at a distance of $\sqrt{2}a_0$; see Fig. 2 inset and caption. The increased residence time of the molecules on the low-temperature surface allows the weak third-nn attractions to overcome the weak second-nn repulsions, thereby stabilizing their mutual adsorption. Such stabilization can also weaken the intraplanar surface Cu bonds in the $p(2\times 2)\text{S}$ surface and undo the small reconstruction. In this picture of cooperative adsorption, H_2S does not adsorb at 300 K and low impingement because the combined residence time of molecules in the required fourfold sites is too short; i.e., the probability of their being adsorbed in third-nn sites is very small. Further support for invoking cooperative adsorption comes from an independent experiment¹³ in which a comparatively low H_2S exposure but at a *high* impingement rate, i.e., where the probability of mutually populating third-nn sites is increased, produces the $c(2\times 2)\text{S}$ structure even at 300 K. We envision that H_2S adsorption competes with diffusion in forming the $\text{H}_2\text{S}(c)$ precursor state much the same way as $\text{H}_2\text{S}(c)$ dissociation competes with desorption in forming the $c(2\times 2)\text{S}$ structure. The choice of temperature and dosing conditions determines which process will dominate.

In summary, we have used NEXAFS and SEXAFS to make the first direct structural determination of a molecular precursor state in dissociative chemisorption. These

results on a microscopic scale were shown to provide insight into the macroscopic kinetic processes of adsorption, desorption, and dissociation. The information and procedures used here should be applicable to a variety of other systems.

The authors thank E. E. Chaban for skillful technical support and D. R. Hamann and J. C. Tully for helpful discussions. The National Synchrotron Light Source is supported by the U.S. Department of Energy, Division of Materials Sciences and Division of Chemical Sciences (DOE Contract No. DE-AC02-76CH00016).

^(a)Present address: Institute for Solid State Physics, University of Tokyo, Roppongi, Minato-Ku, Tokyo 106, Japan.

¹A. Zangwill, *Physics at Surfaces* (Cambridge Univ. Press, Cambridge, 1988), Chaps. 13 and 14.

²S. Hood, B. H. Toby, and W. H. Weinberg, *Phys. Rev. Lett.* **55**, 2437 (1985); O. M. Becker and A. Ben-Shaul, *Phys. Rev. Lett.* **61**, 2859 (1988); J. W. Evans, *Surf. Sci.* **215**, 319 (1989).

³M. Grunze, M. Golze, W. Hirshwald, H.-J. Freund, H. Pulm, U. Seip, M. C. Tsai, G. Ertl, and J. Kupperts, *Phys. Rev. Lett.* **53**, 850 (1984); U. Höfer, P. Morgan, W. Wurth, and E. Umbach, *Phys. Rev. Lett.* **55**, 2979 (1985).

⁴U. Höfer, A. Puschmann, D. Coulman, and E. Umbach, *Surf. Sci.* **211/212**, 948 (1989).

⁵For example, see J. Stöhr, E. B. Kollin, D. A. Fisher, J. B. Hastings, F. Zaera, and F. Sette, *Phys. Rev. Lett.* **55**, 1468 (1985), and references therein.

⁶M. Maglietta, *Solid State Commun.* **43**, 395 (1982).

⁷A. A. MacDowell, T. Hashizume, and P. H. Citrin, *Rev. Sci. Instrum.* **60**, 1901 (1989).

⁸The low impingement rate derived from the nominal pressure reading (i.e., uncorrected for H_2S ion-gauge sensitivity) is estimated to be $1.7(3.2)\times 10^{13}\text{ cm}^{-2}\text{ s}^{-1}$ at 300 (90) K.

⁹J. C. Boulliard and M. P. Sotito, *Surf. Sci.* **195**, 255 (1988), and references therein.

¹⁰C. C. Bahr, J. J. Barton, Z. Hussain, S. W. Robey, J. G. Tobin, and D. A. Shirley, *Phys. Rev. B* **35**, 3773 (1987).

¹¹H. C. Zeng, R. A. McFarlane, and K. A. R. Mitchell, *Phys. Rev. B* **39**, 8000 (1989).

¹²F. Sette, T. Hashizume, F. Comin, A. A. MacDowell, and P. H. Citrin, *Phys. Rev. Lett.* **55**, 1468 (1988).

¹³R. McGrath, T. Hashizume, A. A. MacDowell, F. Sette, and P. H. Citrin (to be published).

¹⁴S. Bodeur and J. M. Esteve, *Chem. Phys.* **100**, 415 (1985).

¹⁵Static and thermal disorder of the $\text{H}_2\text{S}(c)$ species also affects the amplitude of $\chi(k)$ in Fig. 2(b).

¹⁶P. A. Lee, P. H. Citrin, P. Eisenberger, and B. M. Kincaid, *Rev. Mod. Phys.* **53**, 769 (1981).

¹⁷The diffuse LEED pattern from the $<0.38\text{-ML } c(2\times 2)\text{S}$ surface (i.e., less than 0.5 ML for ideal coverage) is consistent with the formation of small $c(2\times 2)$ islands which evolve from the nonideal 0.22-ML $p(2\times 2)\text{S}$ surface comprised of phase-antiphase domains (see Ref. 9).

¹⁸R. G. Caflisch and A. N. Berker, *Phys. Rev. B* **29**, 1279 (1984).